

Plasma bubble zonal velocity variations with solar activity in the Brazilian region

P. M. Terra, J. H. A. Sobral, M. A. Abdu, J. R. Souza, and H. Takahashi

Instituto Nacional de Pesquisas Espaciais – INPE, Avenida dos Astronautas, 1758, Jardim da Granja, CX. 515, CEP: 12.245-970, São José dos Campos, São Paulo, Brazil

Received: 29 September 2003 – Revised: 24 May 2004 – Accepted: 26 May 2004 – Published: 23 September 2004

Part of Special Issue “Equatorial and low latitude aeronomy”

Abstract. A statistical study of the zonal drift velocities of the ionospheric plasma bubbles using experimental airglow data acquired at the low-latitude station Cachoeira Paulista (Geogr. 22.5° S, 45° W, dip angle 28° S) during the period of October to March, between 1980 and 1994, is presented here. This study is based on 109 nights of zonal plasma bubble velocity estimations as determined from bubbles signatures on the OI 630 nm scanning photometer airglow data. The zonal velocity magnitudes of the plasma bubbles are investigated with respect to solar activity and local time. It is verified that these velocities tend to increase with the solar EUV flux, using the solar 10.7-cm radio flux as a proxy (F10.7). These velocities are seen to be larger during the solar maximum activity period than in the solar minimum period. As to the local time variation, they are seen to peak before midnight, in the 20:30–22:30 LT time frame, depending on the season. The all-data plot based on the 109 nights of airglow experiments shows that the plasma bubble mean zonal drift velocities tend to decrease with local time, but they peak at 22:25 LT, where the velocity magnitude reaches 127.4 ms⁻¹. The zonal drift variations with local time and solar flux are shown in Figs. 1 and 2, respectively.

Key words. Ionosphere (ionospheric irregularities; instruments and techniques) – Atmospheric composition and structure (airglow and aurora)

1 Introduction

The low-latitude ionosphere bears the remarkable phenomena of plasma depletions, or bubbles, which consist of extended regions of depleted F-region plasma. The morphology and dynamics of this phenomenon have been investigated over the past several decades (Hanson and Sanatani, 1973; Weber et al., 1978; Woodman and La Hoz, 1976; McClure et al., 1977; Anderson and Haerendel, 1979; Tsunoda, 1981; Mendillo and Baumgardner, 1982; Tsunoda et al., 1982; Carman, 1983; Rohrbaugh et al., 1989 and many other authors).

The plasma bubbles are generated in the nocturnal F-region from initial ionization perturbations and plasma upward drifts (Kelley, 1989). The first set of observations of plasma bubbles over Brazil (Cachoeira Paulista – Geogr. 22.5° S, 45° W, dip angle 28° S) were reported by Sobral et al. (1980a, b) and Sahai et al. (1981) through the use of airglow 630 nm scanning photometers. The developed plasma bubbles move eastward over the South American sector with velocities of ~ 100 ms⁻¹ (Sobral and Abdu, 1990, 1991; Sobral et al., 1985; Abdu et al., 1985; Pimenta et al., 2003). The zonal drifts of the plasma bubbles result from the vertical polarization electric fields that are generated through complex interactions among the tidal winds, the geomagnetic field and the ionospheric plasma in the F-region. Studies of the plasma bubble zonal drift velocities' behavior have been carried out using several techniques, such as the OI 630 nm monitoring in low-latitude and equatorial localities using all-sky imager and photometer systems (Sobral et al., 1985; Sobral and Abdu, 1990, 1991; Fejer et al., 1985; Basu et al., 1996; Valladares et al., 1996; Taylor et al., 1997; de Paula et al., 2002; Martinis et al., 2003; Pimenta et al., 2003).

Solar heating is responsible for the atmospheric tides, which are primary energy sources for the diurnal and nocturnal plasma motions in the ionospheric domain. The purpose of this work is to carry out a statistical study of the plasma bubbles' zonal drift velocities during a solar cycle over Cachoeira Paulista. These velocities were inferred from scanning photometer OI 630 nm data acquired between 1980 and 1994, allowing, therefore, for a comparison of the velocities during the maximum and minimum solar activity periods. The method used here to infer the zonal drifts velocities is based on the photometric data described by Sobral et al. (1991). The large photometric database provides information highly relevant to this work, since it allows for a comparison of the velocities during the maximum and minimum solar activity periods.

Correspondence to: P. M. Terra
(pedrina@dae.inpe.br)

Table 1. Nights with the smallest ΣK_p during the period of October to March, between 1980–1994, of maximum and minimum solar activity.

SOLAR MAXIMUM (1980–1982/1988–1992)											
January	ΣK_p	February	ΣK_p	March	ΣK_p	October	ΣK_p	November	ΣK_p	December	ΣK_p
27–28/1/1990	7°	13–14/2/1980	4+	12–13/3/1980	2+	1–2/10/1980	5–	14–15/11/1990	2+	6–7/12/1980	7–
23–24/1/1980	10–	10–11/2/1980	7°	22–23/3/1988	6°	24–25/10/1992	5+	25–26/11/1989	3+	5–6/12/1988	7+
13–14/1/1988	13+	11–12/2/1980	8+	9–10/3/1981	8–	31–1/11/1981	9+	13–14/11/1990	6°	18–19/12/1990	10–
28–29/1/1990	13+	17–18/2/1980	12°	20–21/3/1980	9+	2–3/10/1980	10–	15–16/11/1990	6°	8–9/12/1988	10°
17–18/1/1988	14°	16–17/2/1982	13+	13–14/3/1988	10–	15–16/10/1988	11+	29–30/11/1992	11–	7–8/12/1980	12+
5–6/1/1981	18°	9–10/2/1980	20+	23–24/3/1988	10+	25–26/10/1992	14°	3–4/11/1980	11°	17–18/12/1990	12+
17–18/1/1982	18°	3–4/2/1981	22°	16–17/3/1991	13–	13–14/10/1991	15°	8–9/11/1980	13–	20–21/12/1981	13+
18–19/1/1988	18°	14–15/2/1980	24°	18–19/3/1991	14–	23–24/10/1990	16°	6–7/11/1980	13°	22–23/12/1992	16–
19–20/1/1988	19–	21–22/2/1990	25–	10–11/3/1981	15+	2–3/10/1989	17–	20–21/11/1990	13+	4–5/12/1980	16–
1–2/1/1992	21–	15–16/2/1980	27+	19–20/3/1980	16°	3–4/10/1989	19–	26–27/11/1989	17+	19–20/12/1981	18–

SOLAR MINIMUM (1983–1987/1993–1994)											
January	ΣK_p	February	ΣK_p	March	ΣK_p	October	ΣK_p	November	ΣK_p	December	ΣK_p
4–5/1/1987	5+	16–17/2/1985	13+	22–23/3/1985	8°	30–31/10/1984	12+	17–18/11/1987	12+	14–15/12/1993	8–
5–6/1/1987	5+	6–7/2/1986	16°	30–31/3/1987	8+	31–1/11/1986	13+	18–19/11/1987	11–	15–16/12/1987	15°
13–14/1/1986	6+	28–1/3/1987	21+	24–25/3/1987	9°	28–29/10/1986	14+	28–29/11/1984	11+	11–12/12/1993	14+
7–8/1/1983	8°	23–24/2/1987	23°	20–21/3/1985	10–	14–15/10/1985	16°	2–3/11/1986	12°		
7–8/1/1987	9°	22–23/2/1987	25–	25–26/3/1987	11–	27–28/10/1984	16+	19–20/11/1987	21–		
4–5/1/1986	10°	21–22/2/1987	26–	23–24/3/1987	12°	28–29/10/1984	17°	20–21/11/1987	19+		
8–9/1/1983	17–	11–12/2/1983	26–	8–9/3/1983	13–	26–27/10/1987	19°	1–2/11/1986	18°		
3–4/1/1986	17°	16–17/2/1994	29+	10–11/3/1983	13°	30–31/10/1986	23°				
26–27/1/1993	28°	15–16/2/1983	30+	9–10/3/1983	15–	29–30/10/1986	23°				
		16–17/2/1983	33–	28–29/3/1987	18–	15–16/10/1985	23+				

2 Results

The zonal plasma bubbles' velocities concerned here are equal to those of the airglow intensity minima, as obtained by an OI 630 nm scanning ($\pm 75^\circ$ around zenith in the east-west direction) photometer system. Those airglow intensity minima result from the decreased plasma concentration within the bubble. This method was described in detail by Sobral et al. (1991). This study is based on 109 nights of zonal scanning photometer measurements of the OI 630 nm night airglow. The mean sunspot number was used here to arrange the data in two groups: the maximum solar activity period group with mean sunspot number > 94.3 (years from 1980 to 1982 and from 1988 to 1992) and the minimum solar activity group with mean sunspot number < 67 (years from 1983

to 1987 and from 1993 to 1994). The geomagnetic activity and seasonal parameters were chosen so as to minimize their effects on the results. So, the following groupings were adopted: ten nights with the lowest ΣK_p (obtained from: <http://spidr.ngdc.noaa.gov/spidr>) values found in the data set for each month of the minimum and maximum solar activity period (Table 1). Those 24-h ΣK_p values refer to the first day of the nocturnal period of observation. The 109 selected nights of the experiments concerned with this work are shown in Table 1.

The set of data shown in Table 1 (109 nights of experiments) was arranged in four groups, namely a) data obtained in the months of January, February and March, during solar maximum activity; b) data obtained in January, February and March during solar minimum activity; c) data obtained

Table 2. Accelerations and velocities at 20:00 LT and 04:00 LT obtained from Fig. 1.

PERIOD	ACCELERATION (ms ⁻¹ h ⁻¹)	V _i (ms ⁻¹)	V _f (ms ⁻¹)
Jan./Feb./Mar./Maximum (Group a)	-8.5	145.6	77.9
Jan./Feb./Mar./Minimum (Group b)	-9.5	123.4	47.4
Oct./Nov./Dec./Maximum (Group c)	-11.0	149.9	61.6
Oct./Nov./Dec./Minimum (Group d)	-14.2	144.4	31.2

in October, November and December during solar maximum activity and d) data obtained in October, November and December during solar minimum activity. The number of nights of observation of those groups were 59, 38, 54 and 21, respectively. These data were studied with respect to the Solar Flux parameter F10.7 cm, as obtained from: ftp://ftp.ngdc.noaa.gov/STP/SOLAR_DATA/SOLAR_RADIO/FLUX/. Finally, all of the plasma bubbles' zonal drift velocities obtained during the 109 nights of observations were plotted as a function of local time and the F10.7 index.

3 Discussion

Figure 1 shows the mean zonal velocities versus local time obtained each group of experiments described in Sect. 2. The fitted straight lines of Fig. 1 show clearly that the mean zonal drift velocities tend to decrease with local time in all groups. This result can be understood through the electric field polarization of the F-region that drives the nocturnal zonal drift of the plasma in that region. The intensity of this electric field is very intense after sunset and decreases with time because of the reduced neutral wind velocity.

In addition, the fitted polynomial lines of Fig. 1 show the tendency of the mean zonal drift velocities to peak before midnight, which is consistent with Fejer et al.'s (1991) observations. The maximum and minimum velocity magnitudes were: a) $V_{max}=127.8 \text{ ms}^{-1}$ at 22:25 LT; b) $V_{max}=109.2 \text{ ms}^{-1}$ at 21:34 LT and $V_{min}=55.7 \text{ ms}^{-1}$ at 03:10 LT; c) $V_{max}=135.9 \text{ ms}^{-1}$ at 20:57 LT and d) $V_{max}=121.6 \text{ ms}^{-1}$ at 20:24 LT.

The initial and final velocities, as taken from the linear fittings of Fig. 1 at 20:00 LT and 04:00 LT, here represented as V_i and V_f , respectively, were used as reference velocities to estimate the zonal acceleration of the bubbles. Table 2 shows the results for V_i and V_f , and that the zonal velocities were larger toward the solar maximum activity period. This result is consistent with that of Biondi et al. (1991) and can be interpreted by means of Eq. (1) from Martinis et al. (2003):

$$V_\phi = U_\phi^P - \frac{H}{P} V_L - \frac{J_L}{P}, \quad (1)$$

where V_ϕ is the zonal drift velocity, U_ϕ^P is the Pedersen-weighted neutral zonal wind, V_L is the vertical drift velocity, J_L is the integrated vertical current density, and Σ_H and Σ_P

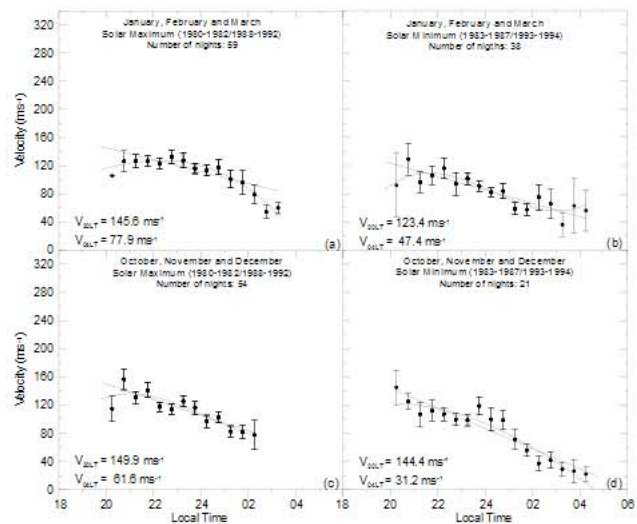


Fig. 1. Zonal velocities of the plasma bubbles versus Local Time for (a) January/February/March solar maximum, (b) January/February/March solar minimum, (c) October/November/December solar maximum and (d) October/November/December solar minimum.

are the total field-line integrated Hall and Pedersen conductivities, respectively. Assuming that the last term of Eq. (1) is small for most local times, except near the solar terminator below the F-region ledge (Eccles, 1998), it is assumed to be null and consequently, the zonal plasma drift velocity will depend essentially on the intensity of the zonal wind velocity U_ϕ^P (Haerendel et al., 1992; Eccles, 1998). So, since during the solar maximum activity the pressure gradients produced by the solar heating are greater and the wind becomes more intense, the zonal plasma drift velocities are expected to be larger in this period as observed in Table 2, where one can also see that shows that the deceleration is consistently higher in spring (October to December) than in summer (January to March) and that the velocities tend to decrease faster with local time during solar minimum than during solar maximum. Since the bubbles' (or plasma) zonal velocities essentially result from the action over the flux tube of the neutral wind system perpendicular to the flux tube, such a faster decrease during spring possibly arises from an equivalent drop in the intensity of the wind system with local time.

Table 3. Velocities' variations with Solar Flux in Jy (where 1 Jy=1 Jansky= 10^{-26} W m⁻²Hz⁻¹= 10^{-4} Solar Flux Units F10.7 cm obtained from Fig. 2.)

PERIOD	VARIATION (ms ⁻¹ (10 ⁴ Jy) ⁻¹)	V _i (ms ⁻¹)	V _f (ms ⁻¹)
Jan./Feb./Mar./Maximum (Group a)	0.05	103.8	110.8
Jan./Feb./Mar./Minimum (Group b)	0.09	85.2	99.1
Oct./Nov./Dec./Maximum (Group c)	-0.05	111.6	103.5
Oct./Nov./Dec./Minimum (Group d)	0.52	92.9	171.6

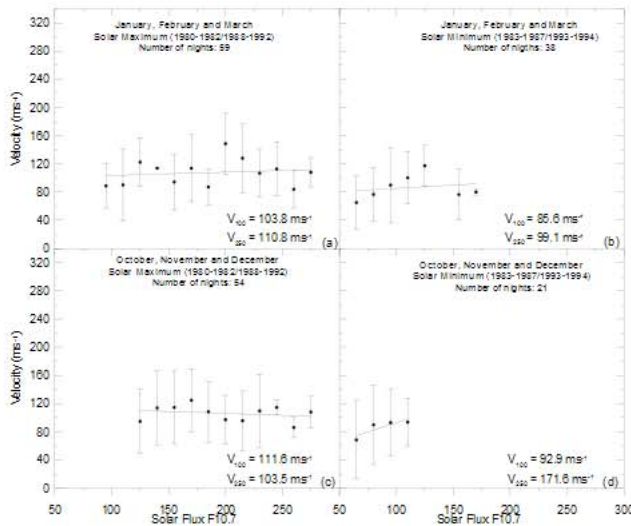


Fig. 2. Same as Fig. 1 except for the Solar Flux F10.7 cm parameter horizontal axis. The plasma bubbles' zonal drift velocities were obtained in the interval between 18:00 LT and 22:45 LT.

It is important to observe that in this analysis it was assumed that both the plasma bubble and the background plasma drift with the same zonal velocity. This is possible since in the fully developed bubbles there is no upward motion (or reduced motion), and its structure becomes strongly coupled to the zonal drifts (Martinis et al., 2003). Figure 2 shows plasma bubbles' zonal mean drift velocities of groups (a) to (d) as a function of F10.7 in the interval between 18:00 LT and 22:45 LT. From Fig. 2 it was observed that, except for panel (c), the mean zonal drift velocities tend to increase with F10.7. This increase is possibly associated with higher pressure/temperature gradients next to the Terminator, resulting in more intense zonal winds during higher F10.7 fluxes. The negative slope of panel (c) corresponds to a velocity drop from 111.6 ms⁻¹ at F10.7=100 to 103.5 ms⁻¹ at F10.7=250, that is, a net drop of only 8.1 ms⁻¹, which is considerably smaller than the magnitude of the error bars, which range from 20 to 100 ms⁻¹. Therefore, this negative slope has hardly any physical meaning.

Table 3 shows the initial and final mean velocities, V_i at F10.7=100 and V_f at F10.7=250, as taken from the least-square fitted lines of Fig. 1. The velocity variations with

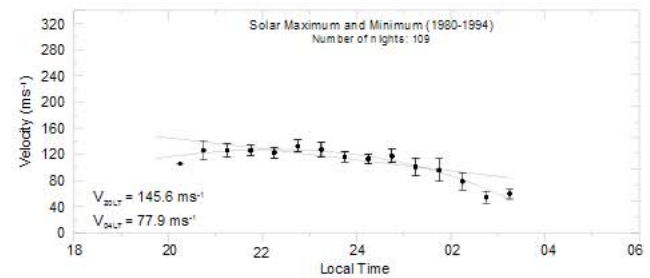


Fig. 3. Plasma bubble zonal drift velocities (109 nights of experiments) versus the Local Time.

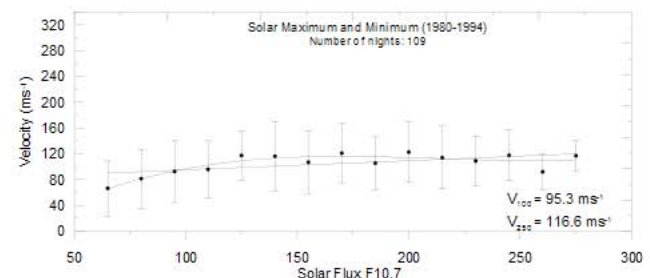


Fig. 4. Plasma bubble zonal drift velocities (109 nights of experiments) versus the Solar Flux F10.7, in the interval between 18:00 LT and 22:45 LT.

F10.7 shown were obtained from V_i and V_f, and the difference between their respective F10.7. The zonal drift velocity increase with F10.7 is clearly larger for group (d), smaller for groups (a) and (b) and slightly negative for group (c).

Figures 3 and 4 show all-data plots of the plasma bubbles' zonal drift velocities obtained during the 109 nights of observations, as a function of local time and the F10.7, respectively. Figure 3 shows that, generally, the mean zonal drift velocities tend to decrease with local time, in agreement with the expected trend. The initial and final mean velocities at 20:00 LT and 04:00 LT on the least-square fitted lines were V_i=145.6 ms⁻¹ and V_f=78.0 ms⁻¹, respectively. The acceleration obtained through V_i and V_f and the time interval between V_i and V_f was -8.5 ms⁻¹h⁻¹. The maximum velocity value found from the fitted polynomial line was 127.4 ms⁻¹ at 22:25 LT. The results pre-

sented in Fig. 4 demonstrate that the plasma bubbles' zonal drift velocities are proportional to F10.7 between 18:00 LT and 22:45 LT. From the linear-square fitting shown in Fig. 4 the mean zonal drift velocities varies from 95.3 ms^{-1} at $F10.7=100$ ($\times 10^{22} \text{ Wm}^2 \text{ Hz}^{-1}$) to 116.6 ms^{-1} at 250 ($\times 10^{22} \text{ Wm}^2 \text{ Hz}^{-1}$).

4 Conclusions

This work concerns the results of a statistical study of the zonal drift velocities of the plasma bubbles using scanning ($\pm 75^\circ$ around zenith in the East-West direction) photometer airglow data acquired at the low-latitude station Cachoeira Paulista (22.5° S , 45° W , dip 28° S), based on 109 nights of experiments during the period of October to March, between 1980 and 1994. It was observed that, generally, the mean zonal drift velocities of the plasma bubbles tend to decrease with local time. This tendency was expected, since the decrease of these velocities with local time, resulting from decreasing neutral wind intensities, is well established. The velocities were observed to peak before midnight, that is, between 22:25 and 21:34 LT during summer (January to March) and between 20:24 and 20:57 LT during spring (October to December). Not only such results are consistent with those of Fejer et al. (1991) for Jicamarca but also the result found here that the deceleration is higher during spring (October to December) than during summer (January to March). The results obtained in this work regarding the variation of the mean zonal velocities with the solar activity showed that these velocities are larger during the solar maximum activity period and tend to increase with F10.7 during the pre-midnight period. Also, it can be observed that these velocities tend to decrease faster with local time during solar minimum than during solar maximum.

Acknowledgements. The authors wish to thank both referees for their comments and acknowledge the supports from the Fundação de Amparo à Pesquisa do Estado de São Paulo – FAPESP through the project 97/14693-3 and Instituto Nacional de Pesquisas Espaciais – INPE and Conselho Nacional de Desenvolvimento Científico e Tecnológico (CNPq) Grants 304494/2003-08 and 520185/95.

Topical Editor M. Lester thanks S. Basu and T. Immel for their help in evaluating this paper.

References

- Abdu, M. A., Batista, I. S., Sobral, J. H. A., de Paula, E. R., and Kantor, I. J.: Equatorial ionospheric plasma bubble irregularity occurrence on zonal velocities under quiet and disturbed conditions from polarimeter observations, *J. Geophys. Res.*, 90, 9921–9928, 1985.
- Anderson, D. N. and Haerendel, G.: The motion of depleted plasma regions in the equatorial ionosphere, *J. Geophys. Res.*, 84, A8, 4251–4256, 1979.
- Basu, S., Kudeki, E., Basu, S., Valladares, C. E., Weber, E. J., Zengingonul, H. P., Bhattacharyya, S., Sheehan, R., Meriwether, J. W., Biondi, M. A., Kuenzler, H., and Espinoza, J.: Scintillations, plasma drifts, and neutral winds in the equatorial ionosphere after sunset, *J. Geophys. Res.*, 101, A12, 26 795–26 809, 1996.
- Biondi, M. A., Meriwether Jr., W. R., Fejer, B. G., Gonzalez, S. A., and Hallenbeck, D. C.: Equatorial thermospheric wind changes during the solar cycle: Measurements at Arequipa, Peru from 1983 to 1990, *J. Geophys. Res.*, 96, A9, 15 917–15 930, 1991.
- Carman, E. H.: Equatorial depletions in the 630 nm airglow at Vanimo, *Planet. Space Sci.*, 31, 335–362, 1983.
- de Paula, E. R., Kantor, I. J., Sobral, J. H. A., Takahashi, H., Santana, D. C., Gobbi, D., Medeiros, A. F., Limiro, L. A. T., Kil, H., Kintner, P. M., and Taylor, M. J.: Ionospheric Irregularity Zonal Velocities over Cachoeira Paulista, *J. Atmos. Solar-Terr. Phys.*, 64, nos. 12–14, 1511–1516, 2002.
- Eccles, J. V.: A simple model of low-latitude electric fields, *J. Geophys. Res.*, 103, 26 699–26 708, 1998.
- Fejer, B. G., Kudeki, E., and Farley, D. T.: Equatorial F-region zonal plasma drifts, *J. Geophys. Res.*, 90, 12 249–12 255, 1985.
- Fejer, B. G., De Paula, E. R., Gonzalez, S. A., and Woodman, R. F.: Average vertical and zonal F-region plasma drifts over Jicamarca, *J. Geophys. Res.*, 96, 13 901–13 906, 1991.
- Hanson, W. B. and Sanatani, S.: Large N_f gradients below the equatorial F-peak, *J. Geophys. Res.*, 78, 1167–1973, 1973.
- Haerendel, G. E., Eccles, J. V., and Cakir, S.: Theory of modeling the equatorial evening ionosphere and the origin of the shear in the horizontal plasma flow, *J. Geophys. Res.*, 97, A2, 1209–1223, 1992.
- Kelley, M. C.: *The Earth's Ionosphere*, International Geophysics Series, 43, Academic Press Inc., 1989.
- Martinis, C., Eccles, J. V., Baumgardner, J., Manzano, J., and Mendillo, M.: Latitude dependence of zonal plasma drifts obtained from dual-site airglow observations, *J. Geophys. Res.*, 108, 1129–1139, 2003.
- McClure, J. P., Hanson, W. B., and Hoffman, J. H.: Plasma bubbles and irregularities in the equatorial ionosphere, *J. Geophys. Res.*, 82, 2650–2656, 1977.
- Mendillo M. and Baumgardner, J.: Airglow characteristics of equatorial plasma depletions, *J. Geophys. Res.*, 87, 7641–7652, 1982.
- Pimenta, A. A., Bittencourt, J. A., Fagundes, P. R., Sahai, Y., Buriti, R. A., Takahashi, H., and Taylor, M. J.: Ionospheric plasma bubble zonal drifts over the tropical region: a study using OI 630 nm emission all-sky images, *J. Atmos. Terr. Phys.*, 65, 117–1126, 2003.
- Rohrbaugh, R. P., Hanson, W. B., Tinsley, B. A., Cragin, B. L., and McClure, J. P.: Images of transequatorial bubbles based on field-aligned airglow observations from Haleakala in 1984–1986, *J. Geophys. Res.*, 94, 6763–6770, 1989.
- Sahai, Y., Bittencourt, J. A., Teixeira, N. R., and Takahashi, H.: Plasma irregularities in the tropical F-region detected by OI 777.4 nm and a 630 nm nightglow measurements, *J. Geophys. Res.*, 86, 3496–3500, 1981.
- Sobral, J. H. A., Abdu, M. A., and Batista, I. S.: Airglow studies on the ionosphere dynamics over low latitude in Brazil, *Ann. Geophys.*, 36, 199–204, 1980a.
- Sobral, J. H. A., Abdu, M. A., Zamlutti, C. J., and Batista, I. S.: Association between plasma irregularities and airglow Brazilian low latitudes, *Geophys. Res. Lett.*, 7, 980–982, 1980b.
- Sobral, J. H. A., Abdu, M. A., and Sahai, Y.: Equatorial plasma bubble eastward velocity characteristics from scanning airglow photometer measurements over Cachoeira Paulista, *J. Atmos. Terr. Phys.*, 47, 895–900, 1985.
- Sobral, J. H. and Abdu, M. A.: Latitudinal gradient in the plasma bubble zonal velocities as observed by scanning 630 nm airglow

- measurements, *J. Geophys. Res.*, **95**, 8253–8257, 1990.
- Sobral, J. H. and Abdu, M. A.: Solar activity effects on equatorial plasma bubble zonal velocity and its latitude gradient as measured by airglow scanning photometers, *J. Atmos. Terr. Phys.*, **53**, 729–742, 1991.
- Taylor, M. J., Eccles, J. V., LaBelle, J., and Sobral, J. H. A.: High resolution OI (630 nm-P1) image measurements of F-region depletion drifts during the Guará campaign, *Geophys. Res. Lett.*, **24**, 1699–1702, 1997.
- Tsunoda, R. T.: Time evolution and dynamics of equatorial backscatter plumes, I. Growth phase, *J. Geophys. Res.*, **86**, A1, 139–149, 1981.
- Tsunoda, R. T. L., Livingston, R. C., Mcclure, J. P., and Hanson, W. B.: Equatorial plasma bubbles: vertically elongated wedges from the bottomside F layer, *J. Geophys. Res.*, **87**, A11, 9171–9180, 1982.
- Valladares, C. E. and Sheehan, R. A.: The multi-instrumented studies of equatorial thermosphere aeronomy scintillation system: Climatology of zonal drifts, *J. Geophys. Res.*, **101**, 26 839–26 850, 1996.
- Weber, E. J., Buchau, J., Eather, R. H., and Mende, S. B.: North-south aligned equatorial airglow depletions, *J. Geophys. Res.*, **83**, 712–716, 1978.
- Woodman, R. F. and LaHoz, C.: Radar observations of F-region equatorial irregularities, *J. Geophys. Res.*, **81**, 5447–5466, 1976.